Creation, Storage, and On-Demand Release of Optical Quantum States with a Negative Wigner Function

Jun-ichi Yoshikawa,[1,*] Kenzo Makino,[1] Shintaro Kurata,[1] Peter van Loock,[2] and Akira Furusawa[1,†]

[1]*Department of Applied Physics, School of Engineering, The University of Tokyo, 7-3-1 Hongo, Bunkyo-ku, Tokyo 113-8656, Japan*
[2]*Institute of Physics, Staudingerweg 7, Johannes Gutenberg-Universität Mainz, 55099 Mainz, Germany*

(Received 13 September 2013; revised manuscript received 14 October 2013; published 13 December 2013)

Highly nonclassical quantum states of light, characterized by Wigner functions with negative values, have been all-optically created so far only in a heralded fashion. In this case, the desired output emerges rarely and randomly from a quantum-state generator. An important example is the heralded production of high-purity single-photon states, typically based on some nonlinear optical interaction. In contrast, on-demand single-photon sources are also reported, exploiting the quantized level structure of matter systems. These sources, however, lead to highly impure output states, composed mostly of vacuum. While such impure states may still exhibit certain single-photon-like features such as antibunching, they are not nonclassical enough for advanced quantum-information processing. On the other hand, the intrinsic randomness of pure, heralded states can be circumvented by first storing and then releasing them on demand. Here, we propose such a controlled release, and we experimentally demonstrate it for heralded single photons. We employ two optical cavities, where the photons are both created and stored inside one cavity and finally released through a dynamical tuning of the other cavity. We demonstrate storage times of up to 300 ns while keeping the single-photon purity around 50% after storage. Our experiment is the first demonstration of a negative Wigner function at the output of an on-demand photon source or a quantum memory. In principle, our storage system is compatible with all kinds of nonclassical states, including those known to be essential for many advanced quantum-information protocols.

DOI: 10.1103/PhysRevX.3.041028 Subject Areas: Photonics, Quantum Physics, Quantum Information

I. INTRODUCTION

Representing flying quantum information, photons are ideally suited for communication between the stations of a quantum network [1,2]. Among various photonic quantum states, single-photon states are the most fundamental, exhibiting a very pronounced negativity of the Wigner function at the origin in phase space. In principle, single-photon-based qubits would allow for scalable quantum computation based on linear-optical circuits, auxiliary quantum states of single and many photons, and photon counters [3,4]. However, nonclassical states beyond single photons such as superpositions of coherent states, exhibiting new forms of Wigner-function negativity, are also expected to be useful for future advanced quantum-information processing [5–12]. One possible strategy to prepare such nonclassical field states is to exploit cavity quantum electrodynamics [13,14] based on a sufficiently strong coupling between single atoms and microwave fields. In an all-optical setting, however, quantum states with a negative Wigner function beyond single photons have been produced solely in a heralded fashion, for instance, using photon-subtraction techniques [15–17]. Here, we propose and experimentally demonstrate an all-optical, heralded creation, storage, and controlled release of nonclassical single-photon states. Moreover, our scheme achieves all these steps by means of a system that can be potentially generalized to accomplish the same tasks for nonclassical states beyond single photons. Most importantly, in our protocol, there is no need to couple a heralded photon into the cavity; the single-photon state is directly produced inside the cavity, and hence coupling inefficiencies for a fragile nonclassical state can be completely avoided.

Single-photon sources are often divided into two types [18], where one corresponds to transitions in electronic energy levels accompanied by a photon emission, and the other is implemented by probabilistically generating photon pairs and detecting one photon and thus heralding another one. The first type of source allows for an on-demand emission of photons, which has been demonstrated with various matter systems [18,19], such as trapped atoms, defects in diamonds, and semiconductor quantum dots. However, these systems typically share a common disadvantage, namely, a very low efficiency for collecting the emitted photons in a specific single spatial mode, and so it remains unclear whether a photon emission has actually happened until the photon is detected [19]. So far, only the class of heralded sources offers high fidelity and flexibility, although at the expense of their intrinsic randomness.

The photon pairs of the heralded sources are typically produced via an optical nonlinearity, namely, either

*yoshikawa@ap.t.u-tokyo.ac.jp
†akiraf@ap.t.u-tokyo.ac.jp

parametric down-conversion [20] or four-wave mixing [21]. Since these optical nonlinearities only require a perturbative coupling between light and matter, heralded photons can be emitted in a well-defined mode with good purity and optical coherence. As a consequence, a negative Wigner function has been observed so far only with this type of source [22,23]. Moreover, measuring parts of a nonlinear optical resource state also allows for the heralded preparation of quantum states beyond single photons or qubits [6–10]. Finally, in contrast to the highly restrictive wavelengths of existing on-demand sources, basically determined by the corresponding energy levels of matter, the heralded approach allows for a broader range of wavelengths, in particular, including the telecom wavelength [24]. Owing to these advantages, the most advanced quantum-information experiments have been demonstrated with such heralded schemes [8–12]. On the negative side, however, since those events when a photon is heralded are totally random and uncontrollable, the probability for creating many such heralded photons simultaneously, as required, for instance, in linear-optical quantum computation [3,4], drops exponentially with the number of photons—unless efficient quantum memories are available.

Therefore, a possible solution to overcome the intrinsic randomness of the heralded schemes is to store a heralded state until it is required [25]. Indeed, single photons were stored in matter systems in previous experiments [26–28]. However, by introducing such buffer memories, some of the disadvantages of matter systems again emerge, such as low photon purity and limited tunability of the optical wavelength (although the memory efficiencies are actually improving [29]). As a remedy, several all-optical experiments have been reported; however, none of them demonstrated high purity [30–34]. Moreover, each had their own additional disadvantages: When the optical delay lines were combined with optical switches, only discrete delays were possible [31]; when the dynamical control of the Q factor of a photonic-crystal nanocavity was successful, the memory time scale was still only subnanoseconds [32–34]. In any case, it appears generally inefficient to first create flying photons and then couple them with stationary memories. In fact, using atomic ensemble memories, Duan *et al.* proposed a scalable quantum repeater with linear optics by smartly unifying the heralding and storage (write-in) processes [35,36]. Our scheme relies upon a similar one-step mechanism, however, in an all-optical fashion, where a heralded photon is created and automatically stored in an optical cavity. After a storage time of up to 0.2 μs, the photon is then released in a controllable fashion and its quantum state reconstructed by homodyne tomography, thus verifying the negativity of the outgoing quantum state. Note that the emission of the single photon is effectively on demand for a time window of approximately 0.1 μs after a random photon-heralding event that occurs, on average, every 3 ms. In order to promote our system to a real on-demand single-photon source, the storage time would have to be increased at least up to this duration of approximately 1 ms, or, alternatively, the photon-generation rate would have to be increased at least up to approximately 1 MHz.

Our scheme for the storage and controlled release of heralded quantum states is based on concatenating two cavities. Although the scheme is experimentally demonstrated for the case of heralded single photons, again, we would like to point out that one of the conceptual innovations here is that our system is potentially extendible to nonclassical states beyond single photons. As a result, we have succeeded for the first time in acquiring, effectively on demand (see above), a quantum feature as strong as the negativity of the Wigner function. This feature is essentially different from the more conventional single-photon character of antibunching [18], which is immune to linear-optical losses and hence valid even for sources with very low purity. The Wigner-function negativity rules out any description in terms of a classical phase-space distribution and thus is important in quantum computing [5]. Moreover, we stress that our system is much more general than a simple photon gun. It is, rather, an all-optical unification of a (potentially continuous-variable, high-dimensional) entanglement generator and a quantum memory. In fact, our heralding mechanism can produce quantum states of light more general than single photons [8–10], and all such states can potentially be stored in our system. In principle, our system may function as a universal quantum memory, where optical, flying quantum information of arbitrary dimension is written into the memory via unconditional continuous-variable quantum teleportation [11,12] and later recalled on demand.

II. WORKING PRINCIPLE

A schematic of our experimental setup with a diagram in the optical frequency domain is shown in Fig. 1. Inside a nondegenerate optical parametric oscillator (NOPO) operating far below threshold, signal and idler photons are probabilistically created and simultaneously appear in different longitudinal modes. We place a shutter cavity (SC) at the exit of the NOPO. Then, a photon inside the NOPO passes through the SC only when it is resonant with the SC, while otherwise it remains inside the NOPO. Therefore, the NOPO concurrently works as a memory cavity (MC). The switch for releasing a photon is quickly realized by shifting the resonance frequency of the SC using an electro-optic modulator (EOM). At first, we set the SC resonant to an idler photon. Any idler photon immediately escapes from the concatenated cavities and is then sent to a photon detector to herald the presence of its partner signal photon inside the MC [Figs. 1(a) and 1(b)]. After the photon creation succeeds, the signal photon can be released by switching the SC whenever wanted [Figs. 1(c) and 1(d)]. Note that an extension of this technique to multiphoton,

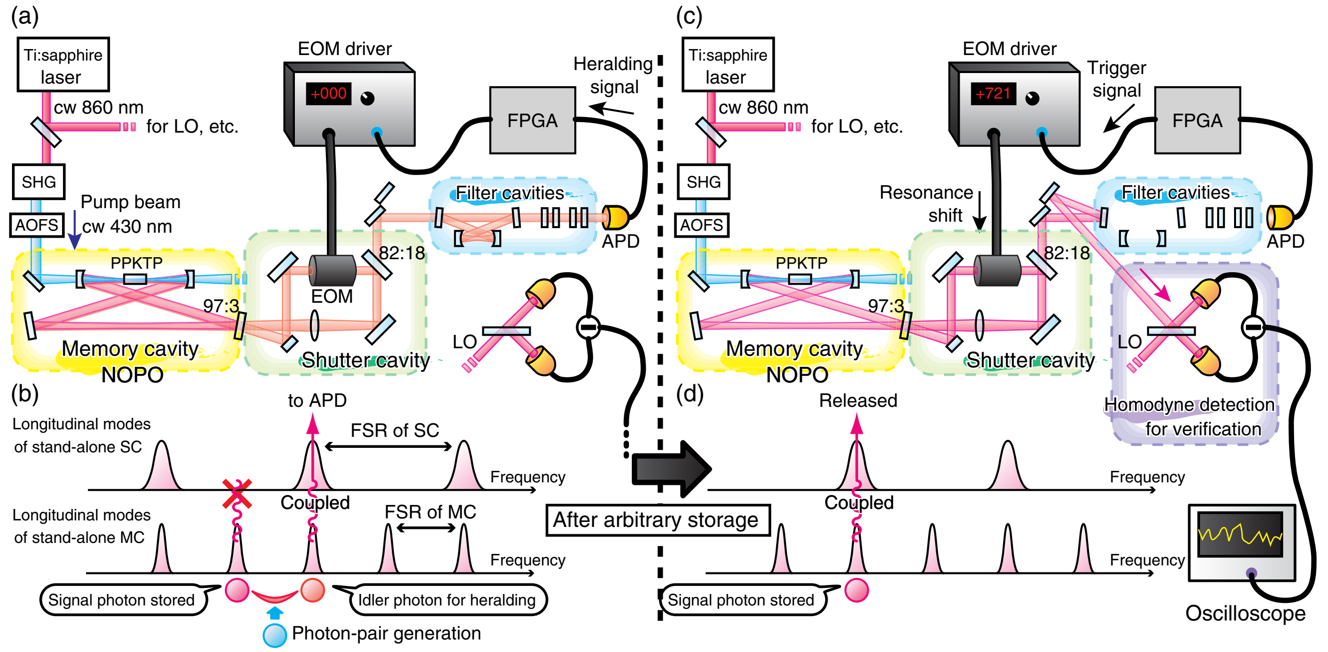

FIG. 1. Schematic diagrams of storage and release. (a) Experimental setup and beam paths at the storage stage. (b) Conceptual diagram in the frequency domain at the storage stage. (c) Experimental setup and beam paths at the release stage. (d) Conceptual diagram in the frequency domain at the release stage. Ti:sapphire, titanium-sapphire laser; cw, continuous wave; SHG, second harmonic generator; AOFS, acousto-optic frequency shifter; APD, silicon avalanche photodiode; and FPGA, field-programmable gate array to process logic signals.

phase-sensitive states appears to be remarkably straightforward [8–10]. Multiple clicks of the photon detector would project the intracavity signal state onto a multiphoton state, and, unlike previous demonstrations without memory [8–10], these clicks would not have to occur simultaneously. Further note that the switching EOM, which is often lossy, is placed outside the MC. This configuration is another reason for the high purity here compared to a previous scheme based on an optical delay loop that contained the switching EOM inside the loop [31].

On a more fundamental level, that intuitive explanation for the high output purity relies on the physics of general coupled systems. More specifically, we may define the damping ratio of the coupled cavities to determine whether they are overdamped or underdamped, which is eventually reflected by the pulse shape of the released single photons. Although this observation is certainly of great interest, it is not directly related to the main experimental achievement to be reported here, which is rather the controlled timing for releasing high-purity single photons. Therefore, we choose to leave the above issue for future works.

Moreover, note that, experimentally, there are actually many longitudinal modes in the NOPO besides the desired signal and idler modes. The real photon detectors are equally sensitive to the photons created in these unused modes. Therefore, in the experiment, we need some frequency filters in order to select only the desired idler mode before the photon detection. Additional optical cavities in the idler line, as illustrated in Fig. 1, can serve this purpose.

The experimental parameters used in our demonstration are described in the following section and in the Supplemental Material [37].

III. EXPERIMENTAL RESULTS AND METHODS

The output quantum states are characterized by optical homodyne detection. Homodyne detection employs interference with a strong local-oscillator light beam, and hence it indicates the photons' coherence and their tunability to some specific wavelength. This situation is in strong contrast to the situation in single-photon verification by antibunching, for which quantum coherence is confirmed by the Hong-Ou-Mandel effect and thus two single-photon creations are necessary [38].

The experimental results are shown in Fig. 2, arranged in an array of rows and columns. The storage time is set to 0, 100, 200, and 300 ns in addition to the intrinsic delay of about 150 ns after the occurrence of the heralding signal, corresponding to columns from left to right.

First, we focus on the leftmost column, corresponding to the intrinsic delay. Figure 2(a) shows the temporal shape of the wave-packet envelope $\psi(t)$ of the released flying photons, which is estimated from the raw data of homodyne detection [39] (details can be found in the Supplemental Material [37]). The horizontal axis is a relative time, where 0 ns corresponds to the events of the idler-photon detection. After opening the shutter at about 150 ns, the wave-packet amplitude suddenly increases and rapidly goes to

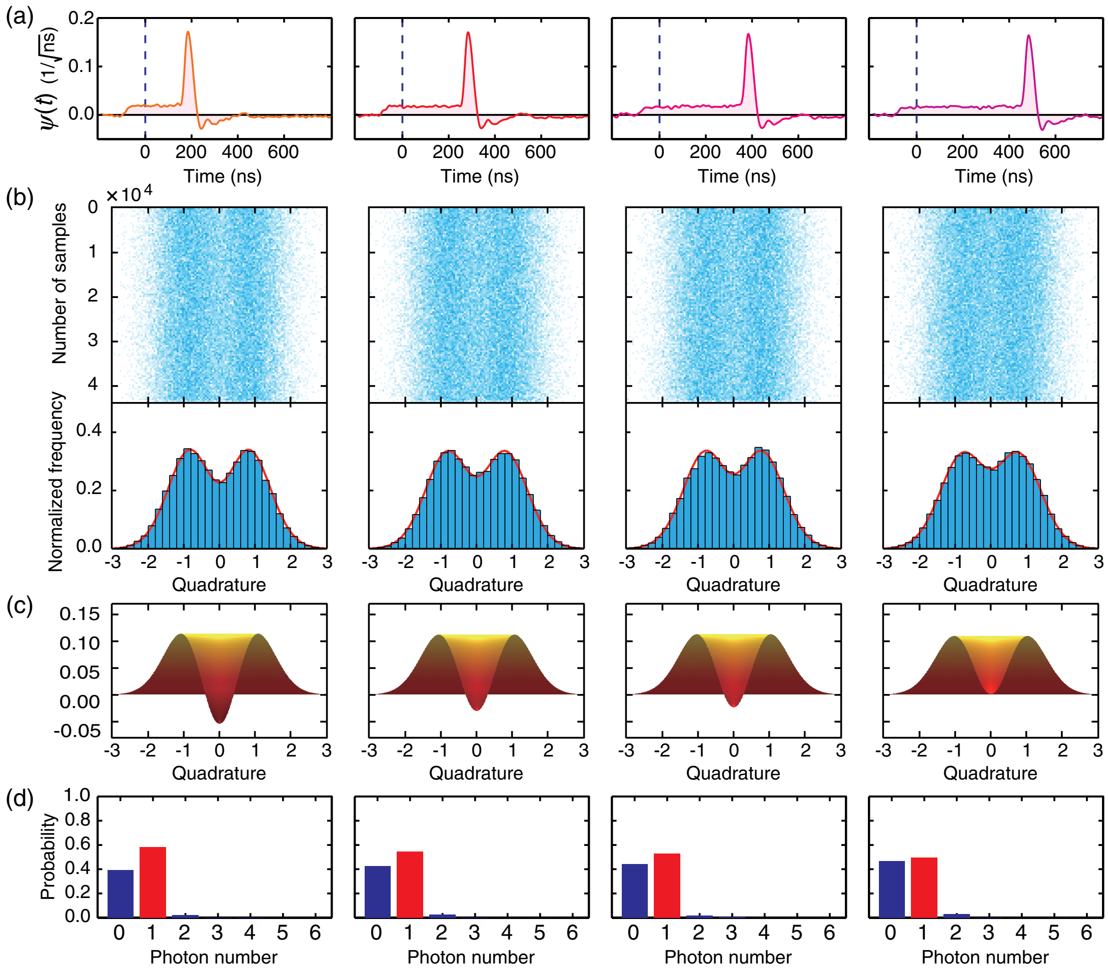

FIG. 2. Experimental results for various storage times. (a) Estimated wave-packet envelopes of the released photons. The idler-photon detection event corresponds to 0 ns. (b) Samples of quadrature amplitudes (upper boxes), their normalized histograms (blue in lower boxes), and their fitting curves (red in lower boxes). The sample number is 4.3×10^4. (c) Sectional side view of the Wigner functions cutting through the phase-space origin. (d) Photon-number distributions. (c) and (d) correspond to the fitting curves in (b). No correction of losses is performed in the data processing. The storage times are 0, 100, 200, and 300 ns, in addition to an intrinsic delay of 150 ns, corresponding to the columns from left to right. The values of the Wigner functions at the origin are -0.054, -0.030, -0.024, and 0.001 from left to right, respectively.

zero, which represents the emission of the photon. The photon pulse width is about 50 ns. In fact, it can be inferred from the experimental parameters that the photon wave packet exhibits damped oscillations (corresponding to underdamping). The damped oscillation is experimentally indicated by the overshoot of the temporal shape down to negative values. Before the photon emission, there are already nonzero values from around -50 ns, showing preleakage. In Fig. 2(b), the quadrature samples and their histogram corresponding to the envelope function $\psi(t)$ are presented. There is a dip at the center of the histogram, which is a characteristic of a single-photon state [22,23]. By performing maximum-likelihood estimation on the quadrature distribution [40], we obtain the Wigner function [Fig. 2(c)] and the photon-number distribution [Fig. 2(d)], where a dip with a negative value of -0.054 for the Wigner function occurs at the phase-space origin as a result of a 58.2% fraction for the single-photon component. Among a total of about 40% photon losses, those coming from the shutter cavity are estimated to be about 15%.

Next, we look at the other panels to see whether the photon wave packet alters its shape and position for longer storages. As shown in Fig. 2(a), the emission times are correctly shifted. However, the shape of the wave packet is independent of the storage time, except for the preleakage. These facts together indicate the success of our demonstration. The single-photon components are estimated as 54.6%, 53.1%, and 49.7%, for 100, 200, and 300 ns, respectively. Although longer storage renders the Wigner function positive, the single photons may still be useful, depending on applications, owing to small multiphoton components [41].

All our results are combined in Fig. 3 for an easy comparison between the envelope function $\psi(t)$ [Fig. 3(a)], its absolute square $|\psi(t)|^2$ [Fig. 3(b)], and the single-photon

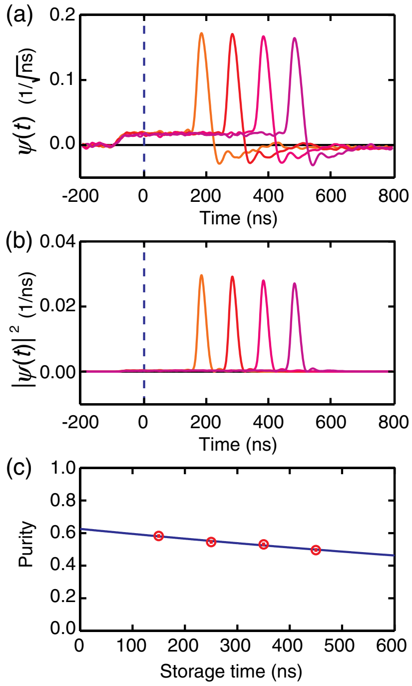

FIG. 3. Experimental dependencies on the storage time. (a) Estimated wave-packet envelopes of the released photons. The storage times are 0, 100, 200, and 300 ns, in addition to the intrinsic 150 ns. (b) Absolute square of the envelopes in (a), proportional to the photon probability density with respect to time. (c) Decay of the single-photon component with respect to the storage time, including the intrinsic delay of 150 ns. The red curves represent the experimental values of 58.2%, 54.6%, 53.1%, and 49.7%, with error bars of ±0.5%. The error is roughly estimated by the bootstrap method [46]. The blue, exponential fitting curve $P(t) = P(0)\exp(-t/\tau)$, where $P(0) =$ 62.6% and $\tau = 1.98$ μs.

component [Fig. 3(c)]. The probability density for the presence of a photon at time t is proportional to the absolute square $|\psi(t)|^2$. From Fig. 3(b), we can infer that the contribution of the preleakage is very small. The lifetime of the photon storage is of the order of 1 μs, as can be seen from the fitting curve in Fig. 3(c), which is comparable with the lifetimes of some ensemble memories [29]. In principle, this lifetime can be further extended by decreasing the intracavity losses. In the following, we will now summarize our experimental methods.

A. Procedure

Our setup is shown in Fig. 1. The source laser is a continuous-wave Ti:sapphire laser with a wavelength of 860 nm. A part of the laser output is frequency doubled to 430 nm, which is used as a pump beam for the NOPO. Two longitudinal modes of the NOPO at 860 nm, separated by a free spectrum range (FSR), are used as the signal and idler. A single longitudinal mode (idler) is selected by filter cavities, and a photon detection projects the twin mode (signal) onto a single-photon state. After some predetermined waiting time, a high voltage of 721 V is applied to the EOM to release the signal photon. It is experimentally essential to avoid above-threshold oscillation at the unused longitudinal modes of the NOPO. The photon-generation rate is about 300 per second with a NOPO pumping power of 3 mW. We want to emphasize that there is a lot of potential for increasing this rate by optimizing the experimental elements such as the filter cavities. The power of the optical local oscillator (LO) is 18 mW, which produces an optical shot noise about 20 dB above the detector's electronic noise.

B. Cavity configuration

The bow-tie-shaped MC contains a periodically poled $KTiOPO_4$ (PPKTP) crystal as a nonlinear medium to operate as a NOPO; it has a round-trip length of 1.4 m (corresponding to the FSR of 2.2×10^2 MHz), where the round-trip optical loss is 0.2%–0.3%. These values determine the photon lifetime. The SC contains a $RbTiOPO_4$ (RTP) EOM for the resonant-frequency shift; it has a round-trip length of 0.7 m, where the round-trip optical loss is 3%. The coupler reflectivity between the MC and the SC is 97%, while that between the SC and the external field is 83%.

C. Verification

While the homodyne detection is a phase-sensitive measurement, the single-photon state is a phase-insensitive state. This phase insensitivity is confirmed by the invariance of the quadrature distribution with the scanned and unscanned phases of the local oscillator. Note that even if there was some phase sensitivity in the released photonic states, becoming manifest in the off-diagonal elements of the photon-number-basis density matrix, it could basically be removed by randomizing the phase of the released wave packets. The photon envelope $\psi(t)$ is determined by the principal-component analysis [37,39]. Each quadrature sample is obtained by a weighted integral of the continuous homodyne data $x(t)$ as $\int x(t)\psi(t)dt$. We assume phase insensitivity when the maximum-likelihood estimation is performed on the quadrature distribution to obtain the photon-number distribution [40]. When we replace the idler beam by an uncorrelated light beam before the photon detection, the observed signal state is almost a zero-photon state, which ensures that the original signal field is indeed conditionally obtained via the idler detection.

Further information on the experimental methods can be found in the Supplemental Material [37].

IV. CONCLUSION AND DISCUSSION

In conclusion, we proposed and experimentally demonstrated the insertion of a quickly tunable cavity at the exit of a NOPO, effectively serving as a kind of quantum memory. After a heralded creation, storage, and on-demand release of single photons with this system, the output states exhibited strong nonclassicality, as became manifest through their negative Wigner functions. Our device works at normal temperature and pressure. In order to function as an on-demand single-photon source, the gap between the photon production rate and the storage time in our system would have to be closed (about 3–4 orders of magnitude).

Our scheme is compatible with hybrid quantum optical experiments, where photon and homodyne detections are employed at the same time, like quantum teleportation [11,12], quantum-information processing [6,7,42], and entanglement distillation [43,44]. Many advanced quantum demonstrations are possible with our system in the future, e.g., the storage and release of multiphoton and/or phase-sensitive states of light [8–10], the controlled interference of many photons simultaneously released from independent memories [3,4,38], and the deterministic transfer of arbitrary quantum optical states into the memories via unconditional continuous-variable quantum teleportation [11,12].

In order to meet the requirements on the quantum nodes for storing quantum information in a standard quantum repeater (approximately 0.01–1 s for approximately 1000 km, depending on the final fidelities), our all-optical system would have to be further improved, since memory times of 0.1–1 μs appear to be insufficient for long-distance quantum communication. Although an increase in lifetime up to the order of seconds, like in nuclear-spin memories, appears unfeasible for our scheme, there is no fundamental reason that prevents our system from achieving those lifetimes currently obtainable with atomic gases at room temperature or with single electronic spins (approximately ms), again corresponding to an improvement of 3–4 orders of magnitude compared to the present experimental demonstration. Experimentally, the most obvious and promising approach to longer lifetimes would be to use longer optical cavities while reducing losses. Moreover, some of the most recent and advanced proposals for implementing a quantum repeater, which include multiplexing and deterministic quantum error correction, have much less-demanding quantum-memory requirements [45].

ACKNOWLEDGMENTS

This work was partly supported by PDIS, GIA, G-COE, and APSA commissioned by the MEXT of Japan, FIRST initiated by the CSTP of Japan, REFOST of Japan, and the SCOPE program of the MIC of Japan. P. v. L. acknowledges support from QuOReP of the BMBF in Germany.

[1] N. Gisin and R. Thew, *Quantum Communication*, Nat. Photonics **1**, 165 (2007).

[2] H. J. Kimble, *The Quantum Internet*, Nature (London) **453**, 1023 (2008).

[3] E. Knill, R. Laflamme, and G. J. Milburn, *A Scheme for Efficient Quantum Computation with Linear Optics*, Nature (London) **409**, 46 (2001).

[4] P. Kok, W. J. Munro, K. Nemoto, T. C. Ralph, J. P. Dowling, and G. J. Milburn, *Linear Optical Quantum Computing with Photonic Qubits*, Rev. Mod. Phys. **79**, 135 (2007).

[5] A. Mari and J. Eisert, *Positive Wigner Functions Render Classical Simulation of Quantum Computation Efficient*, Phys. Rev. Lett. **109**, 230503 (2012).

[6] D. Gottesman, A. Kitaev, and J. Preskill, *Encoding a Qubit in an Oscillator*, Phys. Rev. A **64**, 012310 (2001).

[7] P. Marek, R. Filip, and A. Furusawa, *Deterministic Implementation of Weak Quantum Cubic Nonlinearity*, Phys. Rev. A **84**, 053802 (2011).

[8] E. Bimbard, N. Jain, A. MacRae, and A. I. Lvovsky, *Quantum-Optical State Engineering up to the Two-Photon Level*, Nat. Photonics **4**, 243 (2010).

[9] M. Yukawa, K. Miyata, T. Mizuta, H. Yonezawa, P. Marek, R. Filip, and A. Furusawa, *Generating Superposition of up-to Three Photons for Continuous Variable Quantum Information Processing*, Opt. Express **21**, 5529 (2013).

[10] M. Yukawa, K. Miyata, H. Yonezawa, P. Marek, R. Filip, and A. Furusawa, *Emulating Quantum Cubic Nonlinearity*, Phys. Rev. A **88**, 053816 (2013).

[11] N. Lee, H. Benichi, Y. Takeno, S. Takeda, J. Webb, E. Huntington, and A. Furusawa, *Teleportation of Nonclassical Wave Packets of Light*, Science **332**, 330 (2011).

[12] S. Takeda, T. Mizuta, M. Fuwa, P. van Loock, and A. Furusawa, *Deterministic Quantum Teleportation of Photonic Quantum Bits by a Hybrid Technique*, Nature (London) **500**, 315 (2013).

[13] C. Guerlin, J. Bernu, S. Deléglise, C. Sayrin, S. Gleyzes, S. Kuhr, M. Brune, J.-M. Raimond, and S. Haroche, *Progressive Field-State Collapse and Quanum Non-demolition Photon Counting*, Nature (London) **448**, 889 (2007).

[14] S. Deléglise, I. Dotsenko, C. Sayrin, J. Bernu, M. Brune, J.-M. Raimond, and S. Haroche, *Reconstruction of Non-classical Cavity Field States with Snapshots of Their Decoherence*, Nature (London) **455**, 510 (2008).

[15] A. Ourjoumtsev, R. Tualle-Brouri, J. Laurat, and P. Grangier, *Generating Optical Schrödinger Kittens for Quantum Information Processing*, Science **312**, 83 (2006).

[16] J. S. Neergaard-Nielsen, B. Melholt Nielsen, C. Hettich, K. Mølmer, and E. S. Polzik, *Generation of a Superposition of Odd Photon Number States for Quantum Information Networks*, Phys. Rev. Lett. **97**, 083604 (2006).

[17] K. Wakui, H. Takahashi, A. Furusawa, and M. Sasaki, *Photon Subtracted Squeezed States Generated with Periodically Poled* $KTiOPO_4$, Opt. Express **15**, 3568 (2007).

[18] M. D. Eisaman, J. Fan, A. Migdall, and S. V. Polyakov, *Invited Review Article: Single-Photon Sources and Detectors*, Rev. Sci. Instrum. **82**, 071101 (2011).

[19] G. S. Buller and R. J. Collins, *Single-Photon Generation and Detection*, Meas. Sci. Technol. **21**, 012002 (2010).

[20] S. A. Castelletto and R. E. Scholten, *Heralded Single Photon Sources: A Route towards Quantum Communication Technology and Photon Standards*, Eur. Phys. J. Appl. Phys. **41**, 181 (2008).

[21] J. Fulconis, O. Alibart, J. L. O'Brien, W. J. Wadsworth, and J. G. Rarity, *Nonclassical Interference and Entanglement Generation Using a Photonic Crystal Fiber Pair Photon Source*, Phys. Rev. Lett. **99**, 120501 (2007).

[22] A. I. Lvovsky, H. Hansen, T. Aichele, O. Benson, J. Mlynek, and S. Schiller, *Quantum State Reconstruction*

of the Single-Photon Fock State, Phys. Rev. Lett. **87**, 050402 (2001).

[23] J. S. Neergaard-Nielsen, B. Melholt Nielsen, H. Takahashi, A. I. Vistnes, and E. S. Polzik, *High Purity Bright Single Photon Source*, Opt. Express **15**, 7940 (2007).

[24] S. Fasel, O. Alibart, S. Tanzilli, P. Baldi, A. Beveratos, N. Gisin, and H. Zbinden, *High-Quality Asynchronous Heralded Single-Photon Source at Telecom Wavelength*, New J. Phys. **6**, 163 (2004).

[25] C. Simon *et al.*, *Quantum Memories—A Review Based on the European Integrated Project "Qubit Applications (QAP),"* Eur. Phys. J. D **58**, 1 (2010).

[26] M. D. Eisaman, A. André, F. Massou, M. Fleischhauer, A. S. Zibrov, and M. D. Lukin, *Electromagnetically Induced Transparency with Tunable Single-Photon Pulses*, Nature (London) **438**, 837 (2005).

[27] T. Chanelière, D. N. Matsukevich, S. D. Jenkins, S.-Y. Lan, T. A. B. Kennedy, and A. Kuzmich, *Storage and Retrieval of Single Photons Transmitted between Remote Quantum Memories*, Nature (London) **438**, 833 (2005).

[28] H. P. Specht, C. Nölleke, A. Reiserer, M. Uphoff, E. Figueroa, S. Ritter, and G. Rempe, *A Single-Atom Quantum Memory*, Nature (London) **473**, 190 (2011).

[29] M. P. Hedges, J. J. Longdell, Y. Li, and M. J. Sellars, *Efficient Quantum Memory for Light*, Nature (London) **465**, 1052 (2010).

[30] A. I. Lvovsky, B. C. Sanders, and W. Tittel, *Optical Quantum Memory*, Nat. Photonics **3**, 706 (2009).

[31] T. B. Pittman, B. C. Jacobs, and J. D. Franson, *Single Photons on Pseudodemand from Stored Parametric Down-Conversion*, Phys. Rev. A **66**, 042303 (2002).

[32] Q. Xu, P. Dong, and M. Lipson, *Breaking the Delay-Bandwidth Limit in a Photonic Structure*, Nat. Phys. **3**, 406 (2007).

[33] Y. Tanaka, J. Upham, T. Nagashima, T. Sugiya, T. Asano, and S. Noda, *Dynamic Control of the Q Factor in a Photonic Crystal Nonocavity*, Nat. Mater. **6**, 862 (2007).

[34] A. W. Elshaari, A. Aboketaf, and S. F. Preble, *Controlled Storage of Light in Silicon Cavities*, Opt. Express **18**, 3014 (2010).

[35] L.-M. Duan, M. D. Lukin, J. I. Cirac, and P. Zoller, *Long-Distance Quantum Communication with Atomic Ensembles and Linear Optics*, Nature (London) **414**, 413 (2001).

[36] N. Sangouard, C. Simon, H. de Riedmatten, and N. Gisin, *Quantum Repeaters Based on Atomic Ensembles and Linear Optics*, Rev. Mod. Phys. **83**, 33 (2011).

[37] See Supplemental Material at http://link.aps.org/supplemental/10.1103/PhysRevX.3.041028 for further experimental methods and parameters, and for the explanation of the wave-packet estimation from homodyne signals.

[38] K. Sanaka, A. Pawlis, T. D. Ladd, K. Lischka, and Y. Yamamoto, *Indistinguishable Photons from Independent Semiconductor Nanostructures*, Phys. Rev. Lett. **103**, 053601 (2009).

[39] H. Adbi and L. J. Williams, *Principal Component Analysis*, Comput. Stat. **2**, 433 (2010).

[40] K. Banaszek, *Maximum-Likelihood Estimation of Photon-Number Distribution from Homodyne Statistics*, Phys. Rev. A **57**, 5013 (1998).

[41] R. Filip and L. Mišta, Jr., *Detecting Quantum States with a Positive Wigner Function beyond Mixtures of Gaussian States*, Phys. Rev. Lett. **106**, 200401 (2011).

[42] Y. Miwa, J.-i. Yoshikawa, N. Iwata, M. Endo, P. Marek, R. Filip, P. van Loock, and A. Furusawa, *Unconditional Conversion between Quantum Particles and Waves*, arXiv:1209.2804.

[43] H. Takahashi, J. S. Neergaard-Nielsen, M. Takeuchi, M. Takeoka, K. Hayasaka, A. Furusawa, and M. Sasaki, *Entanglement Distillation from Gaussian Input States*, Nat. Photonics **4**, 178 (2010).

[44] J. Fiurášek, *Distillation and Purification of Symmetric Entangled Gaussian States*, Phys. Rev. A **82**, 042331 (2010).

[45] W. J. Munro, A. M. Stephens, S. J. Devitt, K. A. Harrison, and K. Nemoto, *Quantum Communication without the Necessity of Quantum Memories*, Nat. Photonics **6**, 777 (2012).

[46] B. Efron and R. J. Tibshirani, *An Introduction to the Bootstrap* (Chapman and Hall, New York, 1994).